Earth, Moon, and Planets (2007) 100:1–16
DOI 10.1007/s11038-005-9062-6

Comet Ikeya-Zhang (C/2002 C1): Determination of the Rotation Period From Observations of Morphological Structures

F. MANZINI
SAS, Stazione Astronomica, 28060, Sozzago, Novara, Italy
G. SCHWARZ
DLR, Wessling, Germany
C. B. COSMOVICI
IFSI/INAF, Roma, Italy
C. GUAITA*, L. COMOLLI, A. BRUNATI and R. CRIPPA
GAT, Via Baracca 66, 21047, Tradate, Varese, Italy

(Received 2 July 2004; Accepted 19 November 2005)

Abstract. High quality CCD images obtained at two different observatories in North Italy allowed the identification of four morphological structures near the nuclear region of the comet Ikeya-Zhang (I-Z): haloes, jets, shells and spirals. The interpretation of the nature of these structures has been attempted by means of a comparison of different up-to-date image processing techniques, which led to a single common estimate of the rotation period ($p = 1.48 \pm 0.20$ days).

Keywords: Comets, Ikeya-Zhang, haloes, jets, rotation period, shells, spirals

1. Introduction

The determination of the rotation period of a comet on the basis of morphological studies is a very difficult task, since it may be done only through a continuous monitoring of the cometary jets, and it is dependent on their geometry.

The study of the evolution of prominent jets and shells in the inner coma of comet Hale-Bopp allowed us to discover a strict correlation with the rotation of the nucleus (Manzini et al., 1997; Schwarz et al., 1997; Sekanina, 1998). Comet Ikeya-Zhang was found particularly suitable for similar morphological studies; it was very close to the Sun at the beginning of the observations (March 20, 2002) and to the Earth at the end (April 28, 2002) (Tables I and II).

* E-mail: c.guaita@libero.it

TABLE I

Recording parameters of the observations of Comet P153/Ikeya-Zhang (C/2002 C1) at GAT observatory, Lat. = 45.7388° N, Long. = 8.8996° E

Day	GAT telescope	UT time interval	Number of images	Scale (arcsec pix^{-1})	Scale (km pix^{-1})	Earth Dist. (AU)	Earth Dist. (10^6 km)	Sun Dist. (AU)	Sun Dist. (10^6 km)	Elong. (°)	Phase angle (°)
20 Mar 02	1	18.40–19.15	50	0.995	565	0.7827	117.1	0.5098	76.3	30.4	98.6
21 Mar 02	1	18.24–19.02	50	0.995	551	0.7641	114.3	0.5124	76.7	30.3	100.8
22 Mar 02	1	18.54–19.24	40	0.995	538	0.7458	111.6	0.5161	77.2	30.3	102.8
23 Mar 02	1	18.47–19.22	50	0.995	525	0.728	108.9	0.5208	77.9	30.3	104.8
24 Mar 02	1	18.48–19.31	60	0.995	513	0.7105	106.3	0.5267	78.8	30.4	106.5
25 Mar 02	1	18.41–19.16	50	0.995	500	0.6935	103.8	0.5334	79.8	30.6	108.1
26 Mar 02	1	18.40–19.23	60	0.995	489	0.677	101.3	0.5411	81.0	30.8	109.5
28 Mar 02	1	18.41–19.23	50	0.995	466	0.6455	96.6	0.5591	83.6	31.3	111.8
29 Mar 02	1	18.44–19.20	60	0.995	455	0.6305	94.3	0.5693	85.2	31.8	112.6
31 Mar 02	1	19.08–19.45	50	0.995	434	0.6021	90.1	0.5917	88.5	32.9	113.7
02 Apr 02	1	18.59–19.34	50	0.995	415	0.5758	86.1	0.6165	92.2	34.3	114.0
17 Apr 02	2	22.48–22.53	5	1.165	370	0.4383	65.6	0.8482	126.9	56.9	97.5
22 Apr 02	2	23.25–00.50	60	1.165	351	0.4155	62.2	0.9323	139.5	67.9	87.6
23 Apr 02	2	22.34–00.04	33	1.165	348	0.4124	61.7	0.9488	141.9	70.2	85.6
24 Apr 02	2	22.55–00.27	65	1.165	344	0.4076	61.0	0.9833	147.1	75.1	83.5
27 Apr 02	2	22.11–01.27	210	1.165	342	0.4049	60.6	1.0165	152.1	79.8	77.0

TABLE II
Recording parameters of the observations of Comet P153/Ikeya-Zhang (C/2002 C1) at SAS observatory, MPC code A12

Day	UT time interval	Number of images	Scale (arcsec pix^{-1})	Scale (km pix^{-1})	Earth Dist. (AU)	Earth Dist. (10^6 km)	Sun Dist. (AU)	Sun Dist. (10^6 km)	Elong. (°)	Phase angle (°)
11 Mar 02	18.26–18.42	10	1.96	1361	0.9589	143.5	0.5363	80.2	31.8	80
31 Mar 02	18.42–19.25	35	1.96	853	0.6012	89.9	0.5918	88.5	32.9	113.7
01 Apr 02	18.50–19.20	30	1.96	835	0.588	88	0.604	90.4	33.5	113.9
02 Apr 02	18.48–19.15	30	1.96	816	0.5749	86	0.6167	92.3	34.3	114
03 Apr 02	19.03–19.27	31	1.96	799	0.5627	84.2	0.6298	94.2	35.2	114.9
17 Apr 02	02.42–03.28	60	1.96	629	0.4434	66.3	0.8325	124.5	55	97.6
18 Apr 02	02.59–03.21	30	1.96	622	0.438	65.5	0.8491	127	57	95.8
19 Apr 02	02.25–03.36	36	1.96	614	0.4323	64.7	0.8657	129.5	59.1	94.1
22 Apr 02	22.30–24.00	50	1.96	595	0.419	62.7	0.9161	137	65.7	87.9
27 Apr 02	21.32–00.53	53	1.96	577	0.4064	60.8	1.0006	149.7	77.5	77.3
14 May 02	23.48–01.25	50	1.96	668	0.4709	70.4	1.3027	194.9	118.6	43.2

The favourable geometric conditions of the appearance and the good spatial resolution of our instruments allowed us to study the effects of the interaction between the Sun and the comet just after the perihelion, which led to the enhancement of prominent jets and other cometary structures.

An in-depth analysis of the features described in this paper, performed after extensive image processing with different methods, made it possible to determine for the first time the rotation period of comet I-Z.

2. Observations and Results

2.1. Instrumentations and methods

Three different series of images of comet I-Z were taken at:

(1) the GAT Observatory with a 0.2 m (f/9.3) SCT reflector equipped with a ST7-CCD camera (Kodak CCD KAF-0401E) without filters (March and April 2002) (Table I).
(2) the GAT Observatory with a 0.25 m (f/6.4) Simak reflector equipped with a Hi-SIS43-CCD camera (Kodak CCD KAF-1600) without filters (April 2002) (Table I).
(3) the S.A.S. Observatory with a 0.4 m (f/5) Cassegrain reflector equipped with a Hi-SIS33 CCD camera (Thomson CCD TH7895M), without filters (March and April 2002) (Table II).

The same instruments were successfully used for previous studies on the comet Hale-Bopp (Manzini et al., 1997; Schwarz et al., 1997) and permitted a spatial resolution sufficient to investigate the inner coma morphology.

The comet was observed during 15 consecutive nights from March 20 to April 3, 2002, plus seven further nights in April 2002 and one night in May, 2002. Up to 60 CCD frames were collected during each observation session.

All CCD images were first processed by applying conventional methods of data reduction (bias, dark and flat-field images, that were always collected on the same night of the observation sessions). Further processing was performed by means of the Larson-Sekanina algorithm (Larson and Sekanina, 1984) and by other image processing techniques as described below (see paragraph 3).

To maximize the signal-to-noise ratio, whenever possible, we treated co-added images taken on the same night, instead of processing every single one. The time-lag between our co-added images never exceeded 20 min.

We validated this procedure after verifying that all the details visible in the co-added images were the same as and in the same position of those in every single frame. The smearing effect of the structures consequent to their relative temporal displacement, in our analysis was virtually null (o absent).

2.2. The cometary activity: shells

The I-Z cometary activity was generated from a main jet coming up near the position angle of 270° (with a symmetrical jet at a PA of about 180°) and from minor jets with different position angles and variable intensity over time (Figures 1–3). The position angle of the main jet remained quite constant for more than 10 days (March 20–31, 2002): this jet seemed to show and develop the characteristics of a *porcupine jet* (Manzini et al., 1997).

From animations performed with images taken on the same night and on the following nights, in the period from March 20 to April 4, 2002, we were able to observe an anti-clockwise rotation of the structures surrounding the cometary nucleus.

Starting from March 24, 2002, we observed a shell structure (Hale-Bopp type) superimposed on the main jet, that became more visible in the following days: this finding may indicate, as for comet Hale-Bopp, that the northern rotation pole was progressively turning toward the Earth direction (Lardière et al., 1999). The shell structure was already present also before this date, although it was not completely resolved and remained visible until the first few days of April. The jet producing these shells was probably located near one of the rotation poles of the comet (Sekanina and Boehnhardt, 1997).

Our best CCD images of the jet and shell structures and of the inner coma morphology were acquired at the S.A.S. observatory in the night of March 31, under very good seeing conditions (Figure 3).

Two symmetrical porcupine jets were clearly visible in these images: their axis of symmetry was likely to coincide with the projected direction of the rotation axis of the comet; they can be considered maybe as a fan structure produced by a jet located near one of the rotation poles of the comet (Sekanina, 1998).

2.3. The cometary activity: haloes

The activity of I-Z was highly variable. This was shown on our images by a set of sunward expanding structures ('haloes') (Hergenrother et al., 2002), easily visible in front of the cometary nuclear region.

We observed up to four arc-shaped structures at a time that appeared different on each of the observation sessions. Some of these arc-shaped structures appeared as a result of the perspective overlapping of two or more

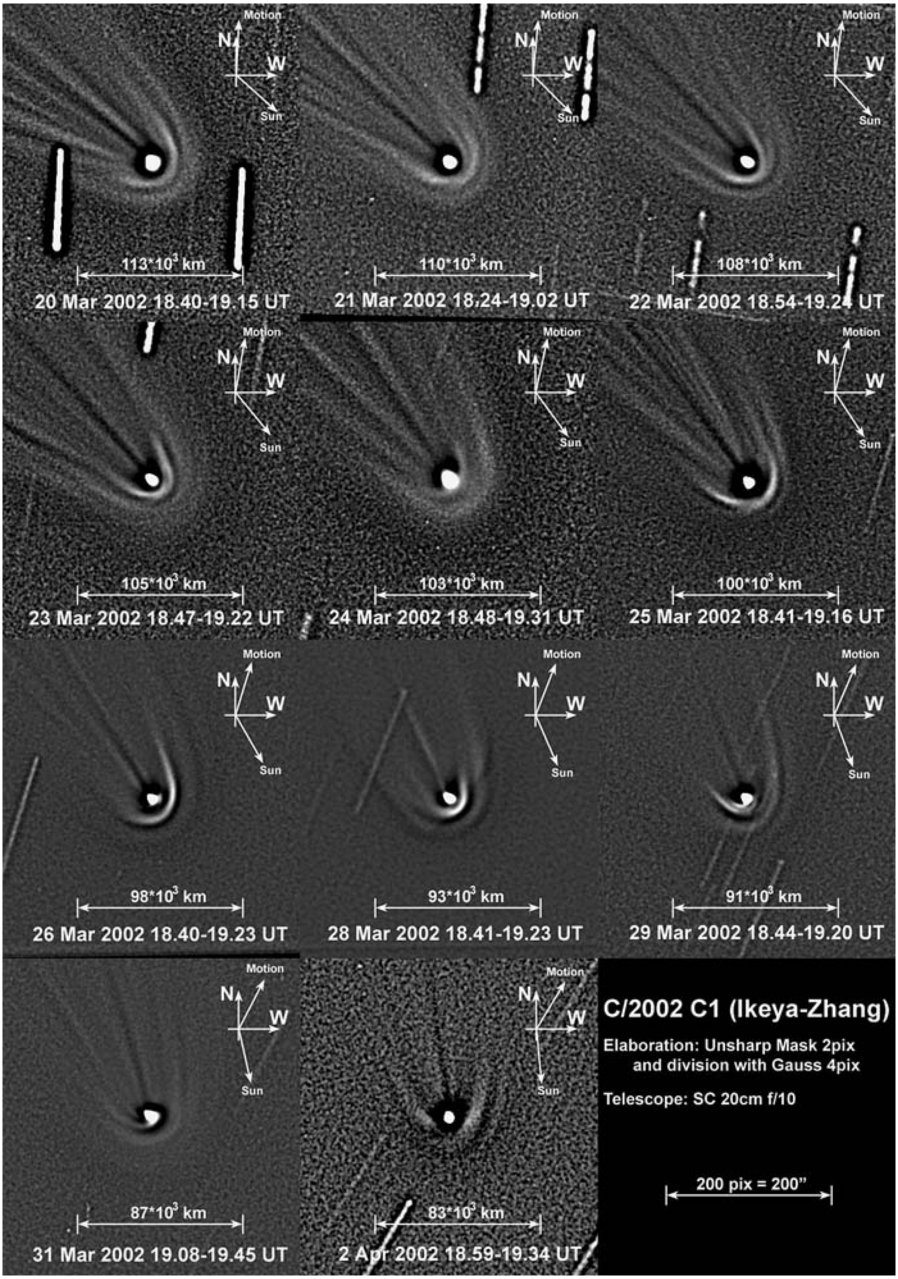

Figure 1. Time evolution of haloes from March 20 to April 2, 2002. The haloes on the sunward side of the comet, easily visible at the beginning of March, disappear at the beginning of April mainly because of the increasing distance between the comet and the Sun.

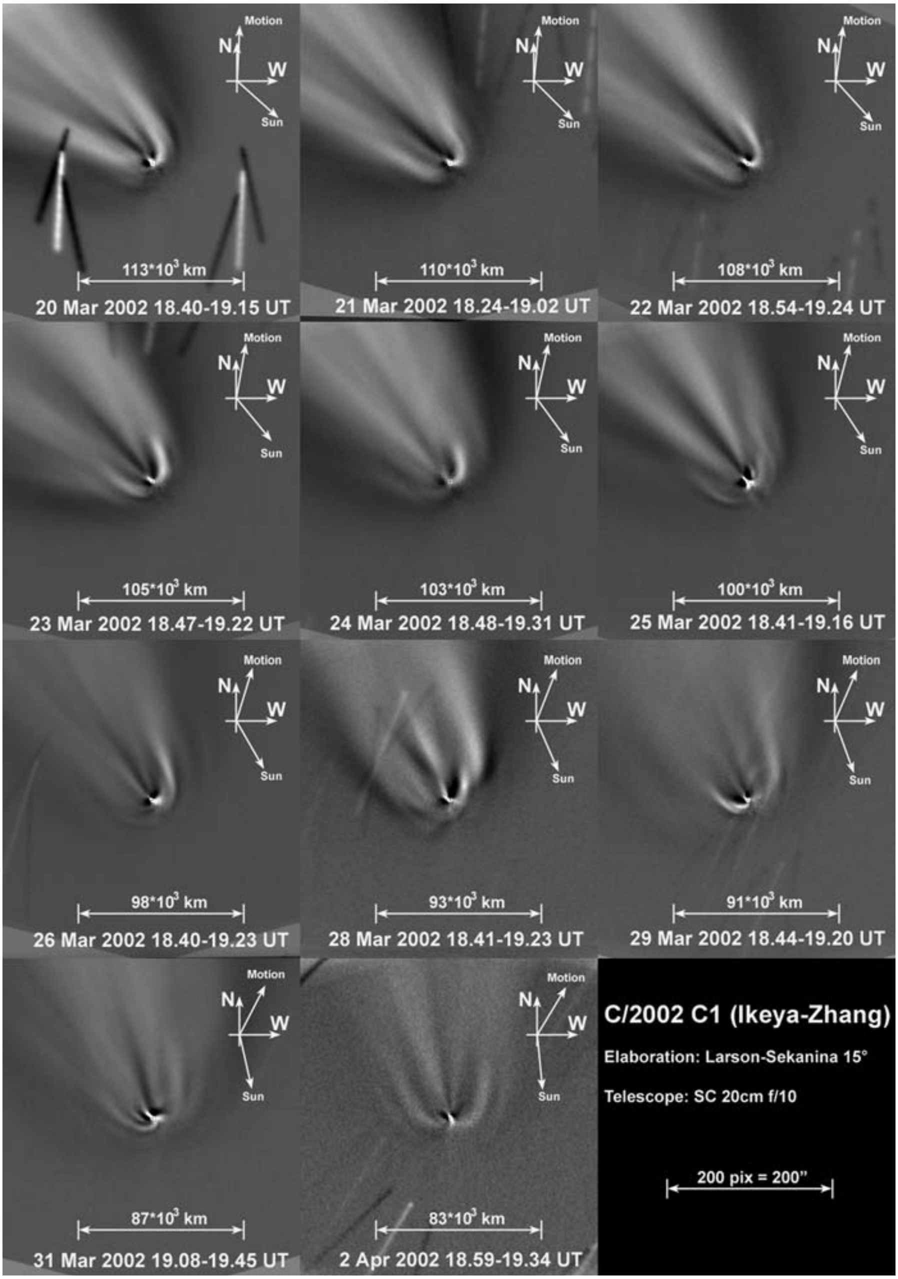

Figure 2. Evolution of jets and other morphological structures from March 20 to April 2, 2002.

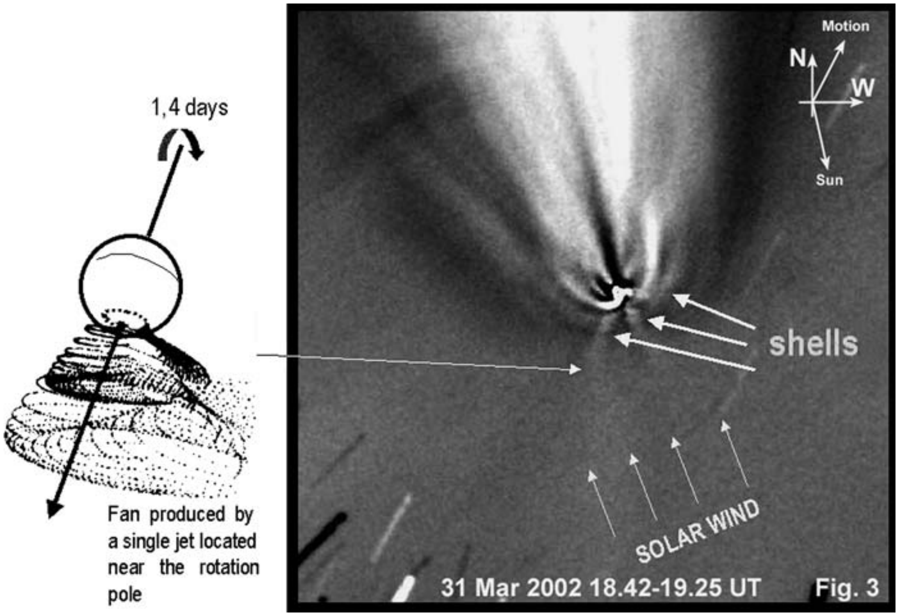

Figure 3. This impressive CCD image of Ikeya-Zhang was acquired at S.A.S. Observatory on March 31, 2002. Thanks to the exceptional seeing conditions, it was possible to clearly confirm the detection of shell structures inside some porcupine jets. Left: a drawing adapted from Sekanina (Sekanina, 1998).

layers of material ejected by simultaneously active jets; sometimes an asymmetric outward displacement was also observed (Figures 1 and 2).

Starting from March 2002 we could observe a relative increase in the brightness of the cometary features, probably originated by a major burst.

In that case, a large amount of material could have enhanced the visibility of some segmentations ('shells') inside the main jet, followed by the formation of a clearly visible halo during the subsequent days.

Since no filters were used, the distinction between neutral, ionic and dusty species was not feasible. In any case the CCD peak sensibility (around 700 nm) favours the dust visibility.

2.4. The rotation period

Based on the evolution of similar shell structures observed inside the porcupine jets of comet Hale-Bopp (Samarasinha et al., 1997), we were able to deduce some important information about the rotation period of the nucleus of comet I-Z also from the shells superimposed on the main jet of comet I-Z.

In particular, we focused our attention on the evolution and the mutual distance of the shells near the cometary nucleus, during two consecutive nights on March 25–26, 2002 (Figure 4). We selected 'shells' closer to the nucleus in order to minimize the influence of the solar radiation pressure on their geometry.

On images obtained on March 25–26, 2002 we made a photometric analysis of two intersection lines as large as 40 pixels across the cometary nucleus (their direction is shown in Figure 4). It was thus possible to measure the mean separation l of the shells in pixels and then to convert it into kilometers.

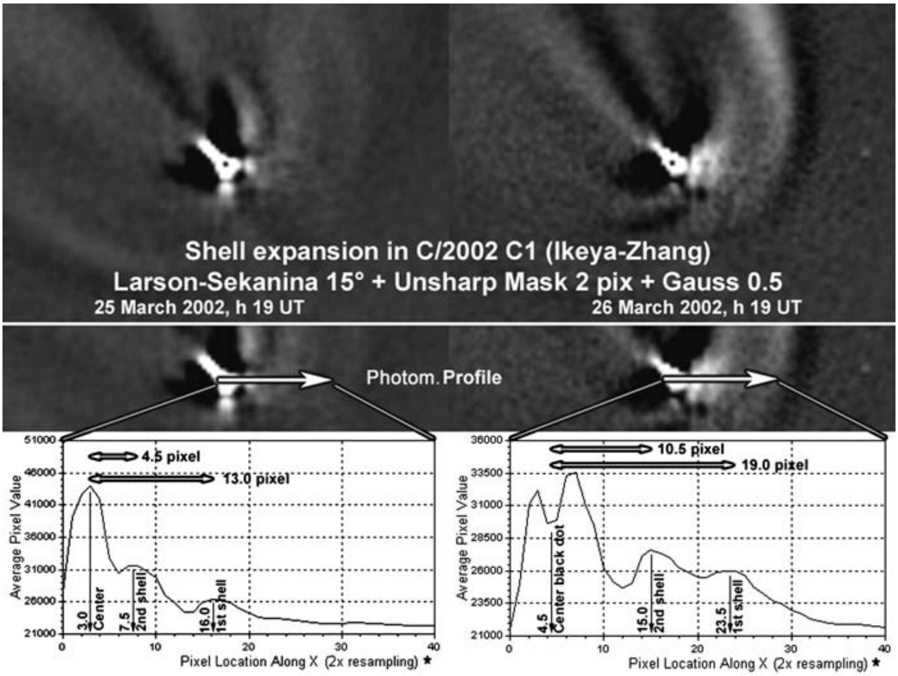

Rotation period calculations					
Day	Nucleus-shell on-plane distance				Image scale
	1° shell	2° shell	1° shell	2° shell	2x spline resampled
	[pix]		[km]		[km pix-1]
25-Mar-02	4,5	13	1125	3250	250
26-Mar-02	10,5	19	2567	4646	245
Expansion rate [km day-1]			1442	1396	
Mean Expansion rate [km day-1]			1419		
Mean Expansion rate [m s-1]			16,4		
25-Mar shell to shell on-plane distance [km]			2125		
26-Mar shell to shell on-plane distance [km]			2078		
Mean shell to shell on-plane distance [km]			2102		
Time period [day]			1,48		

Figure 4. The evolution of a couple of shells at the source of the main jet of comet Ikeya-Zhang, during two consecutive nights (March 25–26, 2002). From the mean separation of the shells and their expansion velocity a nucleus rotation period $p = 1.48 \pm 0.20$ days could be estimated. $^*X$ = chosen photometric section.

Assuming that a new shell formed after every rotation of the comet, the rotational period of the nucleus p, expressed in days, is simply related to the expansion velocity v (km day^{-1}) of the shells (Braunstein et al., 1997) by the relationship:

$$p = i \cdot v^{-1}$$

Based on a shell-to-shell relative distance of 2200 km (measured on the images taken on March 26) and a projected expansion velocity of 1500 km day^{-1} (measured from March 25 at 19 UT to March 26 at 19 UT), a rotation period of 1.48 ± 0.20 days could be derived (Figure 4).

The 'projected' expansion velocity is not affected by the (unknown) inclination of the rotation axis of the comet toward the Earth.

The shells, the subsequent calculations and the derived values are shown in Figure 4.

2.5. Confirmations of the nucleus rotation

A confirmation of the cometary nucleus rotation and of the rotation direction was obtained also by CCD images taken at the S.A.S. observatory on April 17 and 18, 2002.

After the application of an image normalization between all the co-added images obtained during each of these two observation sessions, a large spiral structure around the nuclear position could be observed, probably generated by a previous burst (Figure 5). The slightly elliptical shape of the spiral structure indicated that the rotation axis of the comet was tilted with respect to the Earth by a small angle probably between 0° and 30°.

This structure appeared very similar to the spiral structure observed around the nucleus of comet Hale-Bopp on September 13, 1996 by (Manzini et al., 2001) and (Owens et al., 1999) using the same image processing technique (Figure 5). On that occasion a major burst had led to the wide expulsion of an arc-shaped material that moved across the coma at about 0.35 km s^{-1} and was subsequently scattered.

To further confirm the estimated rotation period, an appropriate radial gradient algorithm was applied to the images taken at SAS Observatory during four consecutive nights (March 31, April 1, 2 and 3, 2002). The angular displacement of the position of the origin of the main jets (maybe near the equatorial region) from the cometary nucleus was clearly identified, in agreement with the rotation previously determined (Figure 6).

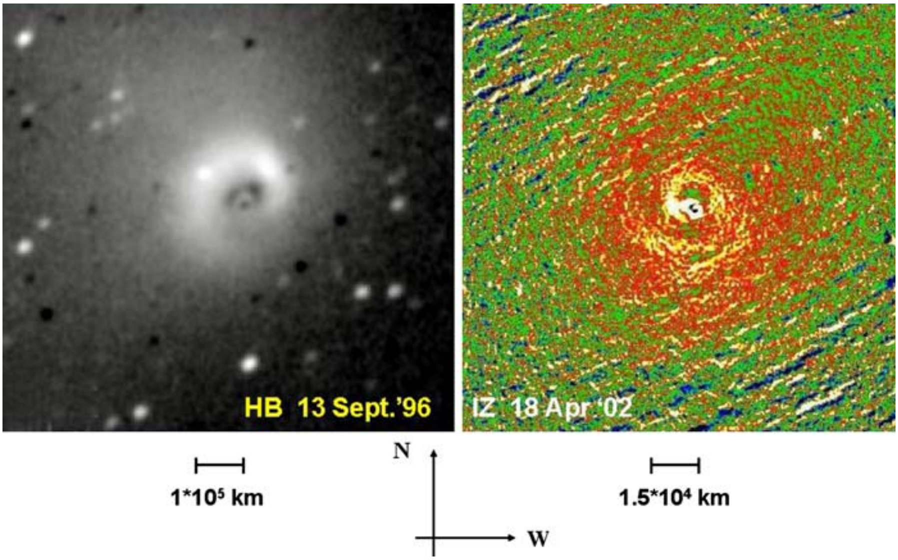

Figure 5. Comets Hale-Bopp and Ikeya-Zhang produced similar helically shaped structures ('spirals'). On the left, a CCD picture of comet H-B taken on September 11–13, 1997 at S.A.S. Observatory (the images were divided to obtain a differential image). On the right, a CCD picture of I-Z obtained on April 17–18, 2002 applying the same image processing.

3. Image Processing Techniques

As shown in the figures, different image processing techniques were used in order to derive the necessary physical parameters from the morphological structures and to determine the cometary rotation period.

3.1. Unsharp masking

A new type of unsharp masking technique was developed to show the haloes in the inner coma of comet I-Z.

The technique consists of the following steps:

- unsharp masking with a 2-pixel radius,
- copy of this image and treatment with a Gaussian blur of 4-pixel radius,
- division of the first image by the Gaussian-blurred copy.

To avoid false interpretation of the series of images, we always used the same processing parameters for all images (Figure 7).

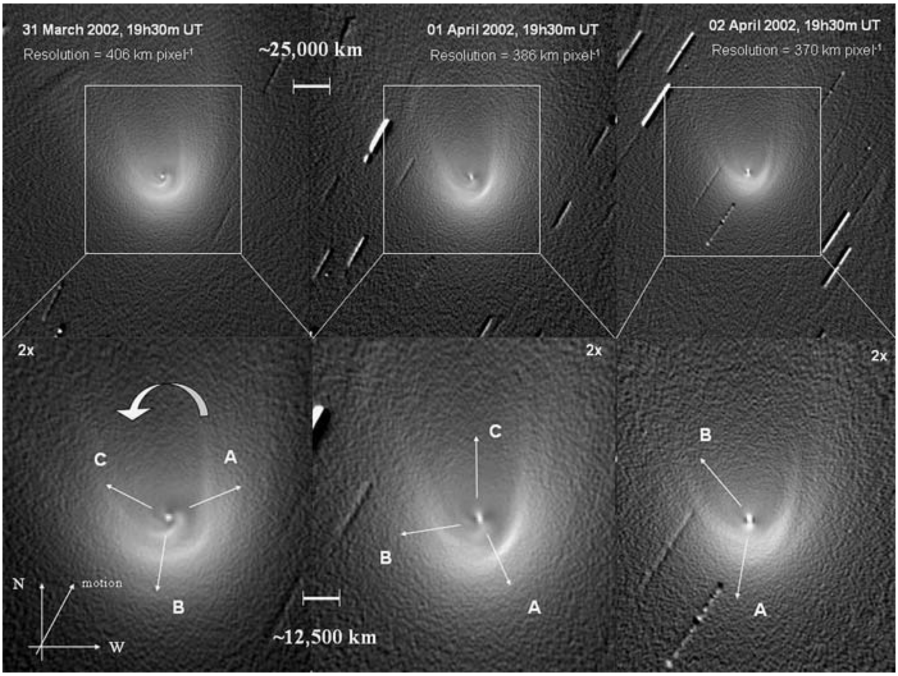

Figure 6. The positions of the main jets from the nucleus of comet Ikeya-Zhang were identified over consecutive days. Their positions are in agreement with the rotation period otherwise determined. The jet named C is not visible in the last image, because of its probable anti-solar position due to the rotation of the nucleus. The processing of the original images is based on the radial gradient.

3.2. Ring masking technique

The most relevant GAT and SAS images were processed with two algorithms:

– a ring masking technique to highlight radial features (i.e. jets)
– a radial de-trending technique to enhance shells and bow shock structures.

In Figure 8, the results of each processing step are shown side by side to allow day by day comparisons.

It should be noted that the GAT and SAS images have different scales and that the seeing conditions at the SAS observatory were exceptionally good.

Our ring masking technique follows the idea that any radial outflow (i.e. jet) leads to slightly enhanced local radiance levels. As these enhanced radiance levels only account for a small percentage of the mean intensity, they are totally invisible without additional image processing.

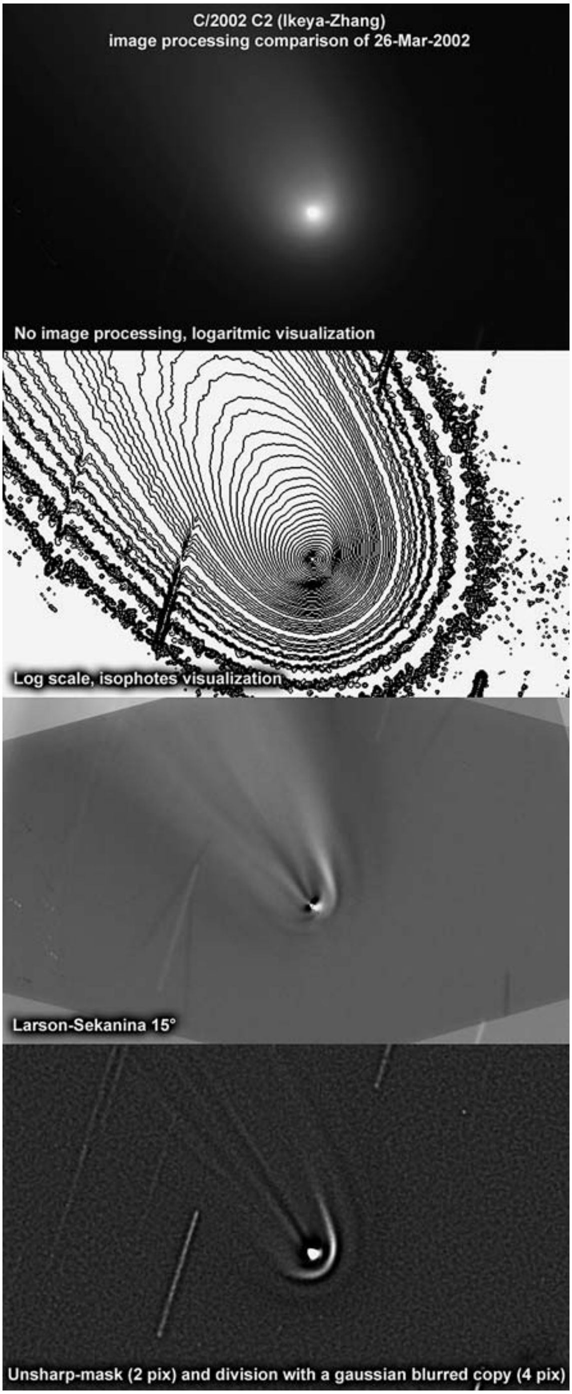

Figure 7. Comparison between unprocessed and processed images.

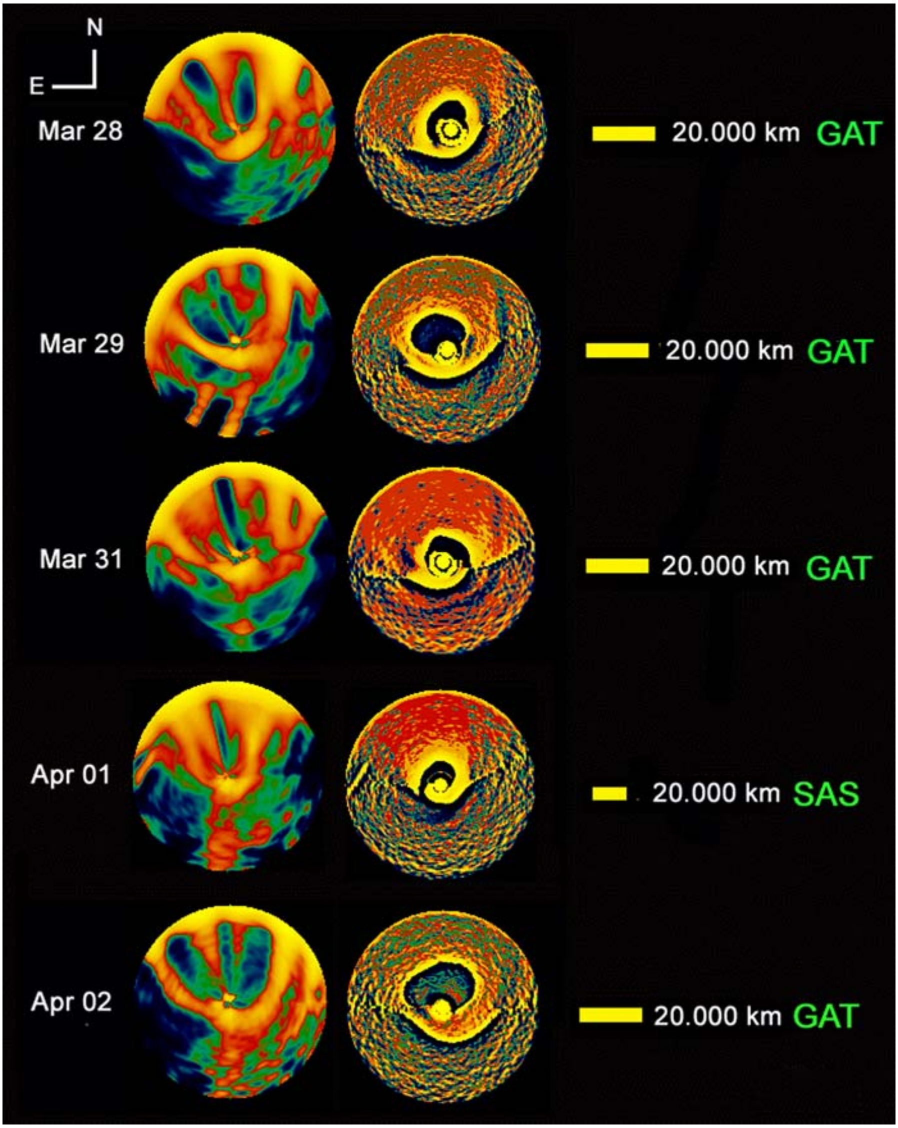

Figure 8. Observations processed with the Ring Masking technique for comparison purposes.

In order to show the differences more clearly, we compare the radiance levels along concentric arcs around the nucleus. In the case of a perfect simmetry, no differences are noticed. On the contrary, if local jet structures result in locally enhanced intensity levels, these differences can be visualized by a number of image processing techniques.

To do this, we selected a ring masking technique by transforming the images into polar co-ordinates around the center of brightness, i.e. the assumed nucleus position.

For more details on the ring masking technique, that was previously successfully applied to comet Halley see (Cosmovici et al., 1988, 1993) and to comet Halley and Hale-Bopp see (Schwarz et al., 1989, 1997).

It should be pointed out that we applied also this technique for comparison in order to obtain a more precise morphological interpretation.

3.3. Radial gradients

Images were investigated with a further method of analysis in order to check the presence of arcs and structures in expansion.

The image processing was carried out as follows:

- the original image was duplicated,
- the duplicate was rescaled by just 1% with respect to its original size,
- the original image and the duplicate were recentered on the comet nucleus,
- finally, the original image was divided by the treated image.

The obtained results are amazing in terms of enhancement of the inner coma structures (Figure 6).

4. Summary

We could study four types of morphological structures inside the inner coma of the comet Ikeya-Zhang:

(a) Sunward-side haloes (Figure 1): they were easily visible starting at the beginning of March 2002 (also in non-processed CCD images) and disappeared at the beginning of April (Hergenrother et al., 2002).
(b) Porcupine Jets (Figure 2): they were almost always present, though weaker, smaller and less evident than those in Comet Hale-Bopp (Boehnhardt et al., 1997).
(c) Shells (Figure 3): sometimes visible inside the porcupine jets as a consequence of their rotation, thus providing basic information on the nucleus rotation period (Manzini et al., 2001). After the detection of impressive shell structures in comet Hale-Bopp (Schwarz et al., 1997), up to now only comet I-Z seems to exhibit such structures. The

detection of shells inside the porcupine jets of I-Z may be considered as a new result for this comet.

(d) Spiral structures (Figure 4) around the nucleus (Owens et al., 1999) as a result of some major bursts and of the geometric conditions of the appearance of the comet I-Z. Their visibility increased in April 2002, possibly because of the position of the rotation axis (nearly radial with respect to the observer).

By applying the methods described above, we were able to determine the rotation period of the nucleus: $p = 1.48 \pm 0.20$ days

References

Boehnhardt, H. et al.: 1997, *Earth Moon Planets* **78**, 179–187.

Braunstein, M. et al.: 1997, *Earth Moon Planets* **78**, 219–227.

Cosmovici, C. B., Schwarz, G., Ip, W. H., and Mack, P.: 1988, *Nature* **332**, 705–709.

Cosmovici, C. B., Schwarz, G., Mack, P., and Maffei, P.: 1993, *An Atlas of Comet Halley as seen from South Africa*, IFSI-CNR, Frascati, Italy.

Hergenrother, C. W. et al.: 2002, *IAUC Circular 7862*.

Lardière, O., Garro, S., and Merlin, J. C.: 1999, *Earth Moon Planets* **78**, 205–210.

Larson, S. and Sekanina, Z.: 1984, *Astron. J.* **89**, 571–578.

Manzini, F. et al.: 1997, *IAUC Circular 6574*.

Manzini, F., Crippa, R., Oldani, V., and Guaita, C.: 2001, *Earth Moon Planets* **87**, 73–85.

Owens, A. et al.: 1999, *Earth Moon Planets* **77**, 293–298.

Samarasinha, N. H., Mueller, B. E. A., and Belton, M. J. S.: 1997, *Earth Moon Planets* **77**, 189–198.

Schwarz, G., Cosmovici, C. B., Mack, P., and Ip, W. H.: 1989, *Adv. Space Res.* **9**(3), 217–220.

Schwarz, G. et al.: 1997, *Earth Moon Planets* **78**, 189–195.

Sekanina, Z. and Boehnhardt, H.: 1997, *Earth Moon Planets* **78**, 313–319.

Sekanina, Z.: 1998, *Ap. J. Lett.* **494**, L121–L124.